Decoupling hydrolysis and mechanical stress effects on Si-MCM-41 relative to hydrothermal stability

López Pérez Lidia[1-2], Melián-Cabrera Ignacio[2], van Eck Ernst[3]

[1]Universidad Autónoma Metropolitana-Azcapotzalco, Departamento de Ciencias Básicas
Avenida San Pablo No. 180. Colonia Reynosa Tamaulipas, México, D.F. CP 02200

[2]University of Groningen, Institute of Technology & Management, Chemical Reaction Engineering, Nijenborgh 4, 9747 AG Groningen, The Netherlands

[3]University Nijmegen, Physical Chemistry, Solid State NMR, Institute for Molecules and Materials, Radboud, Heyendaalseweg 135, 6525 AJ, Nijmegen, The Netherlands

llp@correo.azc.uam.mx

RESUMEN

La estabilidad hidrotérmica del Si-MCM-41 ha sido frecuentemente limitada a la hidrólisis de los enlaces Si-O-Si debido al bajo grado de condensación o al espesor de las paredes de dicho material, o a la combinación de ambos. En este estudio se proporcionan evidencias de un factor adicional, efectos físicos que ocurren durante el secado de un material calcinado que se sometió a un tratamiento hidrotérmico, debido a la tensión capilar ejercida sobre el material cuando el secado se lleva a cabo en medio acuoso. Los resultados fueron interesantes ya que la muestra de material después de ser sometida al tratamiento hidrotérmico a diferente temperatura en agua, presentó desorden completo y contracción de la estructura los resultados revelan que la tensión capilar es responsable del orden perdido y la contracción de la estructura del material a temperatura moderada del hidrotratamiento. Los materiales secados en presencia de solvente de baja tensión superficial preservan su estructura hexagonal y son libres de contracción. Los resultados fueron analizados por diferentes técnicas como: SAXS, TGA, Fisisorción de nitrógeno, ^{29}Si-NMR y TEM.

Palabras clave: Si-MCM-41, estabilidad hidrotérmica, hidrólisis, tensión superficial baja, fuerzas capilares, secado.

ABSTRACT

MCM-41's limited hydrothermal stability has been often related to the hydrolysis of Si-O-Si bonds due to the low degree of condensation or its thin walls, or a combination of them. In this study evidence for an additional factor is provided; a physical effect that occurs during the drying of the hydrothermally treated calcined material, due to the intense capillary stress exerted in water. The results were interesting because the samples gets fully disordered and shrunk at all applied hydrothermal temperatures in water. Comparison between water and low-surface-tension-solvent drying reveals that capillarity is responsible for the loss of ordering (and shrinkage) at moderate hydrothermal temperatures. The material's structure is maintained hexagonal and shrinkage-free under the low-surface-tension-solvent route. The results were analyzed by different techniques as: SAXS, TGA, Nitrogen physisorption, ^{29}Si-NMR and TEM.

Key words: Si-MCM-41, hydrothermal stability, hydrolysis, low surface tension, capillary stress, drying.

INTRODUCTION

The limited hydrothermal stability is considered one of MCM-41's weaknesses, meaning thermal treatments in water or steam, or both. This was yet reported by (Kim and Ryoo, 1996). They reported that MCM-41, and by extension MCM-48, disintegrates in water at temperatures above 343 K; the disappearance of the ordered features was ascribed to hydrolysis and collapse of the structure due to the ill-crystallized thin walls. Such an effect was found to be irreversible and was even observed at room temperature in wet saturated atmospheres (Zhao *et al.,* 1998; Igarashi *et al;* 2003). Cassiers and co-workers reported a systematic study on various types of relevant ordered mesoporous materials under steam; it was found that MCM-41 is the less stable structure under the applied conditions; 30 *vol.%* H_2O at 400 °C for 48 and 120 h (Cassiers *et al.,* 2002).

Research on this area has been greatly dedicated on ways to improve the hydrothermal stability of MCM-41 in two directions; synthetic or post-synthetic routes. On the synthetic approaches, the application of hydrothermal restructuring conditions, meaning water rather than the synthesis mother liquid, was found to enhance the stability significantly. Ribeiro Carrott and coworkers found out that a hydrothermally synthesized material was somewhat more stable than the room-temperature synthesized materials (Ribeiro Carrott *et al,* 1999). Mokaya claimed favourable conditions (423 K for 96 h (Mokaya, 1999) up to 196 h (Mokaya, 2001) in the mother liquid) to have a positive impact on the material's hydrothermal stability, either under steam or boiling water.

The structural disintegration of MCM-41, in water or steam, has been ascribed to the rapid hydrolysis of relatively thin amorphous silica walls. Various factors has been identified to play a role, such as the wall thickness (Cassiers *et al.,* 2002), polymerization degree (Cassiers *et al.,* 2002), cross-linking density associated to the surfactant (Pérez-Arévalo *et al.,* 2002), role of entrapped framework sodium (Pauly *et al.,* 2002) that catalyze the collapse of the structure. Lately the structural stability was correlated to the ratio of the amount of Si-OH to the pore wall thickness (Igarashi *et al.;* 2003).

In this study, the role of the capillary tension during drying, on the calcined materials, that are hydrothermally treated has been investigated. This hypothesis is based on various ideas. First, in a recent study it was demonstrated that the capillary forces play a negative role after chemical detemplating a soft-MCM-41 via Fenton chemistry (López Pérez *et al.,* 2013); if the material after Fenton detemplation is exchanged and dried in a low-surface tension solvent, the structure is well preserved. Other procedures on solvent exchange before drying have been reported for gels processing (Hayashi et al., 1990; Deshpande et al., 1992; Brinker and Scherer,) metal organic frameworks (Eddaoudi *et al.,* 2002; Farha and Hupp, 2010) and mesoporous germanates (Zou *et al.,* 2005), which often collapse and shrink upon solvent removal. Here it is shown that the capillary tension associated to drying, plays a role in the structural loss after the hydrothermal tests of calcined MCM-41, in particular un-aged MCM-41. Thus hydrolysis and capillary tension contribute to some extent to the hydrothermal damage, depending on the type of MCM-41 and the applied hydrothermal conditions (López Pérez *et al.,* 2015).

METHODOLOGY

Synthesis

TEOS based MCM-41 material. The synthesis of this mesophase is based on the method reported by Grün and coworkers (Grün *et al.,* 1999) using tetraethylorthosilicate (TEOS) and ammonia as catalyst without any hydrothermal stabilization. The organic template (cetyltrimethyl-ammonium bromide, CTAB) was dissolved in deionized milli-Q water and aqueous ammonia was added in the following amounts: 2.62 g CTAB, 122 g H_2O and 9.14 g aqueous ammonia (25 *wt.* %, Merck). This was stirred (400 rpm) at 303 K. Around 10 g of TEOS ($Si(OC_2H_5)_4$, Aldrich) were added dropwise in *ca.* 0.5 h using a peristaltic pump (0.3 g/min). A gel with the following molar composition is formed: 1 TEOS: 0.152 CTMABr: 2.8

Revista Tendencias en Docencia e Investigación en Química
Año 2015

Congreso
Internacional de
Docencia e
Investigación en
Química

Azcapotzalco

NH_3: 141.2 H_2O. The material was recovered by filtration and washed with 250-500 mL of milli-Q water and dried overnight at 383 K. The calcination was carried out at 823 K for 5 h in a static-air box furnace at 1 $K.min^{-1}$ heating rate. The template-containing precursor is labelled as Tp while the calcined mesophase is named as Tc, where T denotes TEOS-based.

Hydrothermal treatments

Around 250 mg of the calcined materials was dispersed in 10 mL of water (Milli-Q) and heated to the corresponding test temperature (343, 358 or 373 K), and left for 5 h under gentle stirring. The experiments were carried out using test tubes (Ø=16 mm, L=100 mm). After the hydrothermal test, the excess water was removed by centrifugation at 4000 rpm and the wet material was dried in the test tube at 343 K. Sample dissolution was quantified by weight difference. The resulting material was labelled with the suffix '(temperature.W)'; the temperature is given in Kelvin and W means water-based drying.

Solvent exchange

The wet material after the hydrothermal treatment was washed and exchanged with *n*-butanol (Acros Organics, 99% extra pure) before drying; the sample after the hydrothermal test was centrifuged to remove excess water and washed by centrifugation four times with 5 mL of *n*-BuOH. Each washing step took ~15 min. The drying was carried out in two steps; overnight at 343 K and then the temperature was increased to 373 K and left for 5 h in order to remove the loosely adsorbed solvent residue. The resulting material was labelled with the suffix '(temperature.B)'; the temperature is given in Kelvin and B means *n*-butanol-based drying.

Characterization

Thermogravimetric analysis (TGA) was carried out on a Mettler-Toledo analyzer (TGA/SDTA851e) using a flow of synthetic air of 100 $cm^3.min^{-1}$ NTP. The samples were heated from 303 to 1173 K at 10 $K.min^{-1}$ to verify at which temperature the organic template is removed by calcination.

Small angle X-ray scattering (SAXS) measurements were carried out in a Bruker NanoStar instrument. A ceramic fine-focus X-ray tube, powered with a Kristallflex K760 generator at 35 kV and 40 mA, has been used in point focus mode. The primary X-ray flux is collimated using cross coupled Göbel mirrors and a pinhole of 0.1 mm in diameter providing a CuK□ radiation beam with a full width at half-maximum of about 0.2 mm at the sample position. The sample-detector distance was 1.04 m. The scattering intensity was registered by a Hi-Star position-sensitive area detector (Siemens AXS) in the q-vector range of 0.1–2.0 nm.

Nitrogen physisorption analyses (77 K) were carried out in a Micromeritics ASAP 2420. The samples were degassed in vacuum at 573 K for 10 h. The surface area was calculated using the standard BET method (S_{BET}). The single point pore volume (V_T) was estimated from the amount of gas adsorbed at a relative pressure of 0.98 in the desorption branch. The pore size distributions (PSD) were obtained from the BJH method using the adsorption branch of the isotherms; □$_{BJH}$ represents the position of the maximum. The *t*-plot method was employed to quantify the micropore volume ($V_□$).

^{29}Si solid state NMR spectra were recorded on a 300 MHz Agilent spectrometer operating at a field of 7.05T using a 9.5 mm pencil type MAS probe resonant at 59.596 MHz for silicon and 300.15 MHz for protons. A magic angle spinning at 4 kHz was employed. All spectra were recorded using spinal decoupling at 25 kHz rf-field strength (pulse duration 20 □s and 6° phase). Ramped cross polarisation at a proton rf-field strength of 25 kHz and a 29 kHz rf-field on silicon was employed with 8 ms contact time. Chemical shifts were referenced with respect to tetramethylsilane. To ensure quantitative results, a Si T_1 measurement via cross polarization was recorded. The intensities of the Q_2, Q_3 and Q_4 lines were obtained as a function of the recovery time by deconvoluting the series of spectra with the line parameters obtained by a good S/N CP-MAS spectrum. Typical T_1 values varied between 30 up to 712

Revista Tendencias en Docencia e Investigación en Química
Año 2015

Congreso
Internacional de
Docencia e
Investigación en
Química

s. These T_1 values were used to correct the intensities of the Q-species that were obtained in a direct polarization experiment with a waiting time of 900 s. The results have an estimated accuracy of 0.5 %. The concentration of silanols relative to the total Si is calculated according to (Igarashi *et al.*, 2003).

A combined method (NMR with probe molecules-based IR) was proposed by (Ide *et al.*, 2013) which distinguishes accessible from total bulk silanols; the observed deviation between total and accessible silanols for MCM-41 was relatively small, so we think that method proposed by (Igarashi *et al.*, 2003) is acceptable for our interpretation, and allows relative comparison between the samples.

RESULTS AND DISCUSSION

The calcined MCM-41 mesophases were evaluated regarding the hydrothermal stability by treatments in liquid water at various temperatures ranging 343-373 K. For the TEOS-based material (T*c*), the 100 main reflection drops considerably with the applied temperature and nearly disappears at 373 K (Figure 1). The secondary SAXS features disappear already at 343 K (Fig. 1, inset). These SAXS results are consistent with previous studies in liquid water for a material combining TEOS/silica gel (Kim and Ryoo, 1996), water vapour at room temperature (Igarashi *et al.*, 2003) and 40% steam at 400 °C (Cassiers *et al.,* 2002) (the latter studies are based on purely TEOS-derived materials), which reported XRD or textural reduction. The T*c* material showed dissolution ranging from 0.1 to 2.9 *wt.*%. Quantification of the Si-OH groups (López Pérez et al., 2015) shows that T*c*(343.W) is hydrolyzed when compared to the bare T*c*; it increases from 31.8 (T*c*) up to 44.1 % for T*c*(343.W) while its drops to 27.6 % for T*c*(373.W). The obtained value at 373 K is then 4.2% absolute units lower than that for T*c*. This may be due to condensation reactions between adjacent surface Si-OH or to the lower surface area (735 $m^2.g^{-1}$ compared to 1160 $m^2.g^{-1}$ for the calcined material, Table 1) or both effects. A comparable effect has been reported during the formation of xerogels (Deshpande *et al.,* 1992).

The hypothesis of this study supposes that the material is hydrolyzed during the hydrothermal treatment; the hydrolyzed surface is exposed to intense capillary forces during drying in the cylindrical pores that are able to shrink the structure when this is not mechanically rigid. Hence the collapse is not only associated to hydrolysis, but also to the fact that water has a relatively high surface tension. Calculation of the capillary pressure by the Young-Laplace equation (De Gennes *et al.,* 2003) for the T*c* material, as example, having cylindrical pores of 2.7 nm, assuming a contact angle between water and silica of 45° and pure water ($\square\square$= 71.95 mN.m^{-1}) (CRC Handbook, 2011) reveals that the adhesion pressure within the walls is 745 atm. Such a pressure can mechanically deform the structure when the material is not stable enough.

Table 1. Textural properties (N_2 at 77 K) of TC based MCM-41 materials after hydrothermal stability tests in water or after n-BuOH exchange

Material	S_{BET} (m^2.g^{-1})	V_T (cm^3.g^{-1})	$\square_{BJH}$ (nm)
T*c*	1160	0.858	2.7
T*c*(343.W)	1026	0.549	2.1
T*c*(343.B)	1100	0.613	2.1
T*c*(358.W)	809	0.427	*broad*, max. < 2.0
T*c*(358.B)	1168	0.632	2.1
T*c*(373.W)	735	0.649	*broad*
T*c*(373.B)	797	0.545	*broad*

Revista Tendencias en Docencia e Investigación en Química
Año 2015

Congreso
Internacional de
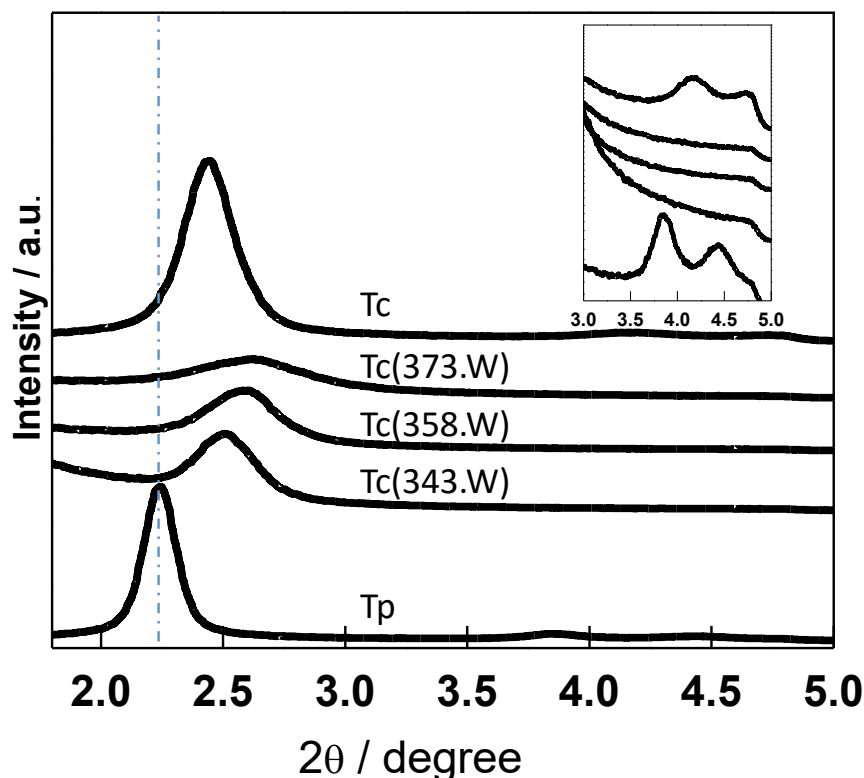Docencia e
Investigación en
Química

Figure 1. *SAXS patterns for the MCM-41 based materials after hydrothermal conditions at 343, 358 and 373 K. Mesophases (Tp) and calcined (Tc) materials are included for comparison. Insets: secondary 110 and 200 reflections, following the same sample order than in the main graphs. Dot lines correspond to the 100 reflection of the template-containing precursors (López Pérez et. al., 2015)*

A way to reduce the capillary stress could be by replacing water by a low-surface-tension solvent and drying the wet solid in that solvent. The solvent must fulfil other requirement such as having a higher boiling point than water, in order to evaporate water preferentially before the mesoscopic menisci are formed. If the boiling point would be lower than water, the pores can get enriched in water during the evaporation and the capillary forces will eventually appear. These conditions are fulfilled by *n*-BuOH (López Pérez *et al.,* 2013); the boiling point is 18 K higher than water while the calculated surface tension (*ca.* 260 atm) is ~0.4 times lower than water; beneficial for reducing the capillary stress.

The calcined un-aged TEOS based material shows the most remarkable improvement. Less shrinkage is found and the intensity of the 100 reflection is much more intense when compared to the water-dried counterparts (Figure 2). The secondary reflections are detected at 343 and 358 K, materials T*c*(343.B) and T*c*(358.B), while those reflections are absent in water (Figure 2-a and –b, insets). At 373 K the secondary reflections are not observed either in water or *n*-BuOH (Figure 2-c, inset), meaning that the structure is converted from hexagonal into wormhole.
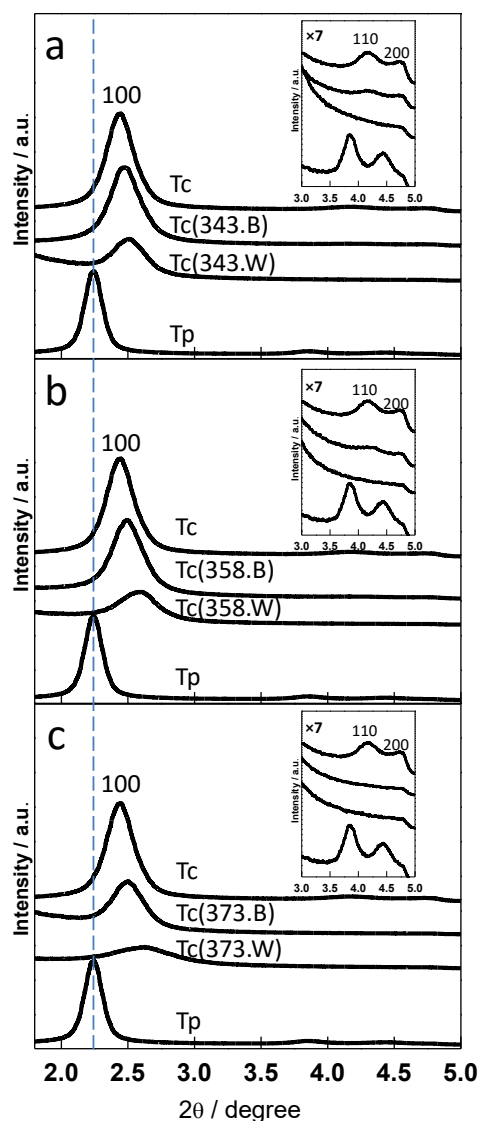
A **U**
Azcapotzalco

Revista Tendencias en Docencia e Investigación en Química
Año 2015

Congreso
Internacional de
Docencia e
Investigación en
Química

Figure 2. *Effect of the n-BuOH exchange on the structural ordering for the **TEOS**-based MCM-41 materials after aqueous hydrothermal conditions at **(a)** 343, **(b)** 358 and **(c)** 373 K. Calcined and mesophase are included for comparison. Insets: secondary 110 and 200 reflections, following the same sample order than in the main graphs. Dot line corresponds to the 100 reflection of the template-containing precursor (Tp), (López Pérez et. al., 2015)*

The un-aged TEOS-based materials were further studied by gas adsorption since they showed the most remarkable SAXS-based results in terms of structural preservation. The N_2 gas adsorption isotherms are shown in Figure 3 and the derived textural parameters are given in Table 1. The calcined Tc sample shows the typical reversible isotherm characteristic of MCM-41, with a sharp capillary condensation at around 0.2-0.3 in the relative pressure (p/po). This corresponds to a relatively sharp pore size distribution centred at 2.7 nm in the BJH plot (Figure 3-a, right). No microporosity was detected. The BET surface area and pore volume account 1160 $m^2.g^{-1}$ and 0.858 $cm^3.g^{-1}$.

Treatment in water at 343 K, Tc (343.W), has a marked reduction of the capillary condensation at 0.2 p/po (Fig. 3-a, left) that corresponds to a much flatter pore size distribution (Fig. 3-a, right). Consequently the pore volume drops to 0.549 $cm^3.g^{-1}$. The BET surface area remains relatively high with 1026 $m^2.g^{-1}$ because the pores are smaller (2.1 nm) due to the shrinkage. The *n*-BuOH-exchanged material, Tc

Revista Tendencias en Docencia e Investigación en Química
Año 2015

Congreso
Internacional de
Docencia e
Investigación en
Química

(343.B), has a steeper capillary condensation and a more defined (*i.e.* more intense) pore size distribution, centered at 2.1 nm. The surface area and pore volume of this material increases when compared to the water-dried counterpart, with 1100 $m^2.g^{-1}$ and 0.613 $cm^3.g^{-1}$. These results are in line with the better structural preservation revealed by SAXS when *n*-BuOH was applied, that showed the presence of the secondary reflections.

Concerning the 358 K treated samples (Figure 3-b), the typical MCM-41 isotherm shape is lost when the material is dried in water; the pore size distribution is much broader than the 343 K-water-treated material. The surface area and pore volume drops considerably to 809 $m^2.g^{-1}$ and 0.427 $cm^3.g^{-1}$ due to the severe structural collapse as discussed in Fig. 2-b. When *n*-BuOH exchange is applied the textural features are better preserved; the isotherm maintains the capillary condensation and consequently the pore size distribution is relatively narrow (Fig. 3-b, right). The derived textural parameters of this material, Tc (358.B), are relatively high with 1168 $m^2.g^{-1}$ and 0.632 $cm^3.g^{-1}$, compared to the calcined material. The high surface area is due to the smaller pores, centered at 2.1 nm that contribute less to the pore volume but more to the surface area.

At 373 K the isotherms show in both cases (water or *n*-BuOH) no capillary rise at 0.2 p/po and desorption hysteresis with a closure point at around 0.45 p/po (Fig. 3-c, left). This is an indication of pores with wide parts and restrictions. There is no evidence of well-defined mesoporosity in the adsorption pore size distributions (Fig. 3-c, right). The surface areas are the lowest (735 and 797 $m^2.g^{-1}$) and the pore volumes are relatively low, 0.649 and 0.545 $cm^3.g^{-1}$.

The textural characteristics corroborate the observations on the structural changes: intense pore size distributions and high textural parameters, together with well-defined SAXS secondary reflections are found when *n*-BuOH exchange is applied for hydrothermal temperatures below 373 K. At 373 K the hydrolysis leads to a pronounced and irreversible damage.

The SiOH concentration for the Tc(343.B) material was estimated at 41.8 % (López Pérez *et al.,* 2015) that is comparable to the water-dried counterpart, 44.1 % for T*c* (343.W), revealing that the surface is indeed hydrolyzed. When combining NMR, SAXS and textural analyses, it is concluded that the *n*-BuOH-exchanged T*c* (343.B) sample is nearly equally hydrolyzed but it is structurally better preserved because of the lower capillary tension that the material has been subjected.

The TEOS-based material (T*c*) revealed the lowest hydrothermal stability, in terms of hydrolysis and capillarity, when dried in water. Severe shrinkage and loss of hexagonal ordering was found at all temperatures. Shrinkage was progressive with the applied hydrothermal temperature. Remarkably, both ordering and unit cell dimension are preserved when applying the *n*-BuOH route for materials treated at temperatures of 343-358 K; comparison between water and *n*-BuOH reveals that the loss of ordering (*i.e.* conversion of hexagonal into wormhole) at 343 and 358 K (water-based) is not due to hydrolysis but to capillarity. This finding is remarkable since it is often thought that the loss of ordering is attributed to hydrolysis exclusively. This mesostructure suffers from extensive hydrolysis at 373 K, which explains the ordering loss even when dried in *n*-BuOH.
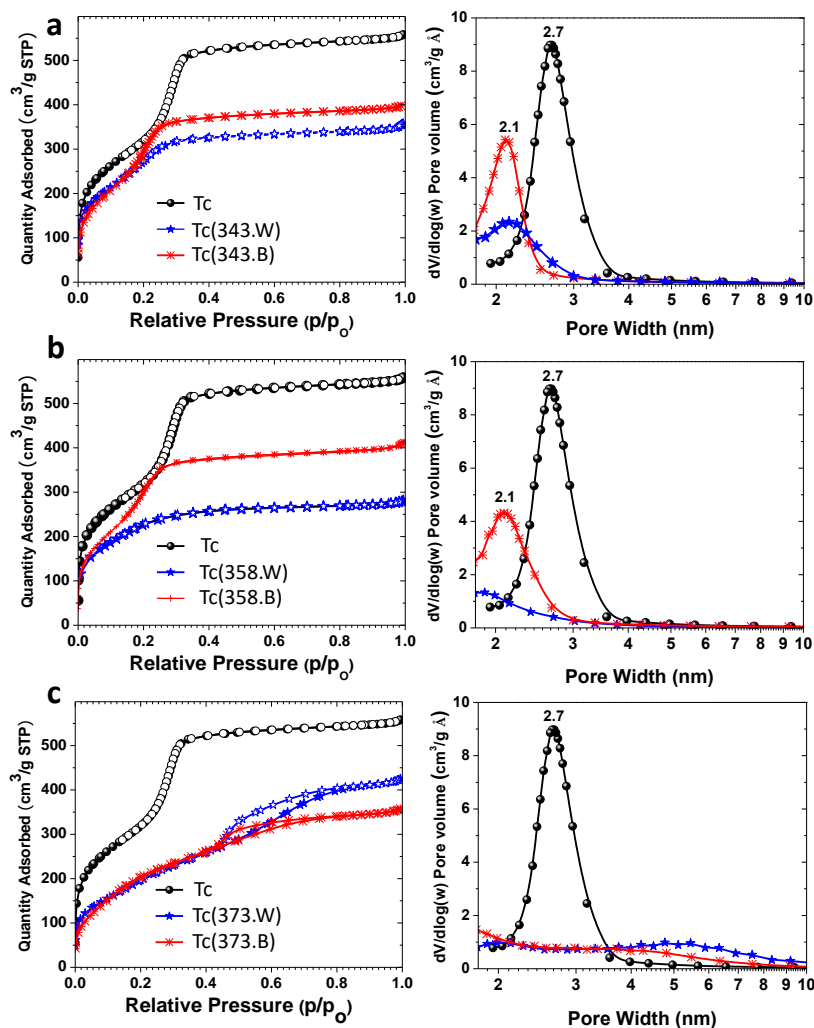
Revista Tendencias en Docencia e Investigación en Química
Año 2015

Congreso
Internacional de
Docencia e
Investigación en
Química

Figure 3. *Nitrogen adsorption isotherms (left) and BJH pore size distributions (right) for the **TEOS**-based MCM-41 materials after aqueous hydrothermal conditions, dried in water or after n-BuOH exchange:*
***a)** 343;* ***b)** 358 and **c)** 373 K (hydrothermal temperature). The calcined material is included for comparison. (López Pérez et. al., 2015)*

In terms of material dissolution, it was generally found that this is higher with the increasing treatment temperature, but there is apparently no correlation with the hydrothermal stability. In fact the less stable material (T*c*) dissolves less.

CONCLUSIONS

Interpretation of hydrothermal stability results of Si-MCM-41 materials have been done considering hydrolysis and capillary stress-induced effects. The latter effect is significantly important when the structure is not mechanically robust, on the pristine material level or upon the hydrothermal conditions. Capillarity can give rise to two effects: shrinkage but also to loss of ordering, during drying in water.

Revista Tendencias en Docencia e Investigación en Química
Año 2015

Congreso
Internacional de
Docencia e
Investigación en
Química

The proposed exchange solvent, *n*-BuOH, shows evidences that capillary effects play a role; however, its surface tension is still moderate. Therefore the exchange/drying effectiveness can be enhanced by reducing the surface tension of the medium further. Another aspect that can play a role is the possible entrapped water, which has not been efficiently extracted with *n*-BuOH.

The un-aged TEOS based mesostructure has the lowest hydrothermal stability, in terms of hydrolysis and rigidity, associated to the lack of ageing step in the synthesis protocol. In *n*-BuOH, well preserved hexagonal structures are obtained at temperatures of 343-358 K, while in water capillarity produces disordered wormhole and shrunk structures. At 373 K hydrolysis is extensive leading to a wormhole structure.

REFERENCES

Brinker C. J. and Scherer G. W. (1990). Sol–Gel Science: The Physics and Chemistry of Sol–Gel Processing, Academic Press Inc., San Diego. Ch 8.

Cassiers K., Linssen T., Mathieu M., Benjelloun M., Schrijnemakers K., Van Der Voort P., Cool P., Vansant E.F. (2002). *Chem. Mater.* 14: 2317.

De Gennes P.G., Brochard-Wyart F., Quere D. (2003). Capillarity and Wetting Phenomena: Drops, Bubbles, Pearls, Waves, Springer.

Deshpande R., Hua D.W., Smith D.M., Brinker C.J. (1992). J. Non-Cryst. Solids. 144: 32.

Eddaoudi M., Kim J., Rosi N., Vodak D., Wachter J., O'Keeffe M., Yaghi O.M. (2002). *Science* 295: 469–472.

Farha O.K., Hupp J.T. (2010). *Accounts Chem. Res.* 43: 1166-1175.

Grün M., Unger K.K., Matsumoto A., Tsutsumi K. (1999). Micropor. Mesopor. Mater. 27: 207.

Hayashi F., Takei K., Machii Y., Shimazaki T. (1990). *Nippon Seram. Kyo. Gak.* 98: 663.

Ide M., El-Roz M., de Canck E., Vicente A., Planckaert T., Bogaerts T., van Driessche I., F Lynen., van Speybroeck V., Thybault-Starzyk F., van Der Voort P. (2013). *Phys. Chem. Chem. Phys.* 15: 642.

Igarashi N., Koyano K.A., Tanaka Y., Nakata S., Hashimoto K., Tatsumi T. (2003). Micropor. *Mesopor. Mater*. 59: 43.

Kim J.M., Ryoo R., Bull R. (1996). *Korean Chem. Soc.* 17: 66.

López Pérez L., Ortiz-Iniesta M., Zhang Z., Agirrezabal-Telleria I., Santes M., Heeres H.J., Melián-Cabrera I. (2013). *J. Mater. Chem.* a 1: 4747.

López Pérez L., van Eck E., Melián-Cabrera I. (2015). Accepted to Microporous and Mesoporous Materials.

Mokaya R. (1999). *J. Phys. Chem.* B. 103: 10204.

Mokaya R., (2001). *Chem. Commun.* 933.

Pérez-Arévalo J.F., Domínguez J.M., Terres E., Rojas-Hernandez A., Miki M. (2002). *Langmuir* 18: 961.

Pauly T.R., Petkov V., Liu Y., Billinge S.J.L., Pinnavaia T.J. (2002). J. Am. Chem. Soc. 124: 97.
Ribeiro Carrott M.M.L., Estêvão Candeias A.J., Carrott P.J.M., Unger K.K. (1999). *Langmuir* 15: 8895.

The CRC Handbook of Chemistry and Physics (2011). 89th edition. CRC Press. 6-149.

Zhao X.S., Audsley F., Lu G.Q. (1998). *J. Phys. Chem.* B. 102: 4143.

Zou X., Conradsson T., Klingstedt M., Dadachov M.S., O'Keeffe M. (2005). *Nature* 437: 716.